# Abstraction of Sketch Features for Predicting Hidden Shapes of Sketches for The Automatic Conversion into 3D Models

Masaji Tanaka[1] , Tetsuya Asano[2] and Chiharu Higashino[2]

[1]Okayamaity University of Science, tanaka@mech.ous.ac.jp
[2]Aikoku Alpha Corporation, {higashino, t-asano}@aikoku.com

Corresponding author: Masaji Tanaka, tanaka@mech.ous.ac.jp

**Abstract.** Sketches in the form of line drawings are important illustrations to directly express the overviews of objects, especially mechanical objects. Numerous methods that automatically convert sketches into 3D models have been proposed. However, no practical system for conversion has been developed till now. Consequently, we have developed a method as SFBCM (Sketch Feature-Based Conversion Method) for this conversion. In SFBCM, when a sketch is input, SFs (Sketch Features) that indicate simple sketches of objects such as cubes, cylinders are detected and extracted as 3D features step by step. Consequently, a 3D model can be obtained by combining them based on the sketch. However, several issues have remained in SFBCM. Especially, to handle hidden shapes in sketches was an important issue. In this paper, ASF (Abstract Sketch Feature) is introduced for predicting hidden shapes of sketches. Each ASF is a part of an SF. This prediction is based on human perception and enables SFBCM to be simplified drastically. For example, when people look at a sketch of a pole standing on a plate, they think the two objects are contacted centrally, but they can be uncontacted and placed near their edges theoretically. The introduction of ASF can clarify this contact problem. In this paper, ASF for SFBCM is explained in detail with an example, and many other complex examples are described for indicating its effectiveness.

**Keywords:** Abstraction, SFBCM, Abstract Sketch Feature, ASF, Human Perception.
**DOI:** https://doi.org/10.14733/cadaps.2022.977-987

## 1    INTRODUCTION

Sketches in the form of line drawings are commonly observed in magazines, books, manuals, etc. Sketches are also important for designers, especially mechanical designers, when they invent new ideas of products and their parts. The automatic conversion of sketches into 3D models will be advantageous for several applications. Moreover, it is expected that robots will be able to understand sketches by their converted 3D models in the future. In the last fifty years, numerous methods to automatically convert sketches into 3D models have been considered and developed. However, no

real system for the conversion has been developed till now. We have been developing methods for the conversion of sketches to 3D models for approximately eight years. Consequently, we proposed a method as SFBCM (Sketch Feature-Based Conversion Method) to achieve this conversion [16]. Fig. 1 shows three basic SFs (Sketch Features) that indicate a cuboid, cylinder, and round hole.
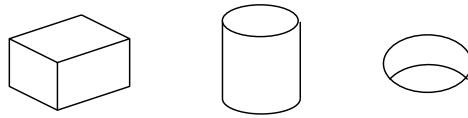


**Figure 1**: Basic three SFs: (a) Cuboid, (b) Cylinder, and (c) Round hole.

In SFBCM, when a sketch is input, the 3D model of it can be obtained by detecting and extracting SFs step by step and combining them. Fig. 2(a) shows Example 1 that is a sketch of a mechanical part. When Example 1 is input to SFBCM, first a cylinder is detected and extracted. Second, a cuboid is detected and extracted. If remained lines can be restored into a cuboid, the 3D model of Example 1 can be obtained. This scene can be seen in Fig. 2(b). However, several issues have remained in SFBCM. Obviously, to handle hidden shapes in sketches is an important issue as shown in the restoration of the cuboid in Example 1. Also, when a person looks at Example 1, he/she thinks that a cylinder and a rectangular column are placed symmetrically and vertically on a plate. However, many solutions as 3D models can exist in theory from that. For example, 3D models of Fig. 2(c) which is a screen shot of solid modeler (SolidWorks) can correspond to Fig. 2(a).
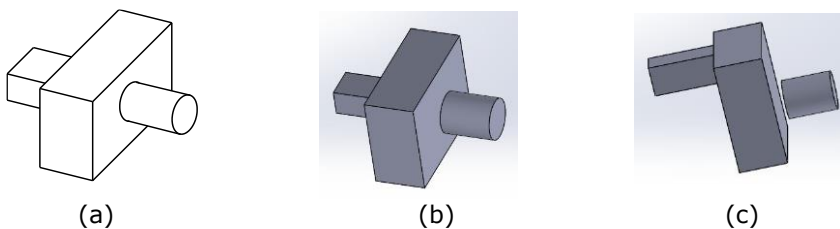


**Figure 2**: Example 1: (a) Example 1, (b) 3D model of (a), and (c) Another 3D models corresponding to (a).

Therefore, it is difficult or impossible to predict exact shapes from hidden shapes in sketches because many solutions can exist despite that there are many hidden shapes in sketches. In our past methods, inductive learning systems were applied to the prediction as restoration processes of SFs [19]. However, generally learning systems seem to be difficult for applying to the prediction because there are too many types of hidden shapes in sketches. Moreover, to collect big data of that will be wasteful and not effective because each data will have to be input by user(s) manually until all target hidden shapes can be predicted exactly. On the other hand, human perception will be effective such as the recognition of Example 1. Therefore, it might be possible to construct a theory of the prediction based on human perception. If the theory is constructed, learning systems will be useless.

In this paper, human perception is applied to the prediction of hidden shapes in sketches for SFBCM. For this application, we attempt to abstract SFs, and ASF (Abstract Sketch Feature) is defined. Each ASF is a part of an SF. Fig. 3 shows two SFs and an ASF separately in Example 1. There are an SF of a cylinder (green), a cuboid (pink), and an ASF (blue). Here, two dotted lines of the pink cuboid are easy to predict in SFBCM. The blue ASF can be predicted as an SF of a cuboid by applying human perception. Consequently, we propose our improved method as ASF for SFBCM in this paper. The rest of this paper is organized as follows. In Section 2, related works of this method is explained. In Section 3, the algorithm of this method is explained in detail with Example 1. In Section 4, three examples are indicated. In Section 5 and Section 6, several issues and the possibility of this method to the future are discussed and conclusion is described.
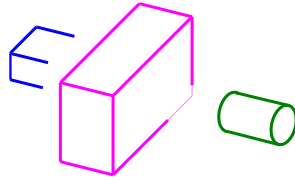
**Figure 3**: Two SFs (cylinder and cuboid) and an ASF in Example 1.

## 2    RELATED WORKS

There are numerous papers on the automatic recognition of sketches in the form of line drawings and/or their conversion into 3D models. Their classification is presented in [6]. The original line labeling technique was developed as Huffman-Clowes labeling, [5],[12]. In this labeling process, the objects of sketches were limited to opaque trihedral polyhedrons, and each sketch was an orthogonal projection of an object viewed from a general position. Each line segment of a sketch was labeled as "+" (convex line), "-" (concave line), or with an arrow (occluding line). From the labeling, the vertices were classified into the following four types of junctions: *L*, *W*, *T*, and *Y*-junctions. This naming was derived from the shapes of the alphabets, i.e., "L," "W," "T," and "Y," respectively. The relationships between the labeling and the junctions were summarized as a junction dictionary. Moreover, Varley et al. [21] handled high-order junctions such as *K*- and *X*-junctions. Although these labeling techniques were applied to sketches consisting of only straight lines, Malik [14] created a junction dictionary for curved lines in sketches. For example, if a straight line segment expresses a limb line of a cylindrical face of an object, it was labeled with double arrows.

Fig. 4 shows the line labeling in Example 1. In Fig. 4(a), each line segment is labeled. Arrowed, double arrowed, "+," and "-" lines are colored blue, pink, red, and green, respectively. From this figure, each junction can be recognized, as shown in Fig. 4(b), by using junction dictionaries. Here, four blue points are *L*-junctions, and two light blue points are *Curvature-L*-junctions [14]. A red point is a *Y*-junctions, and two pink points are Three-Tangent points [14]. In our method, these three points are regarded as *Y*-junctions. Also, four green points are *W*-junctions, and five brown points are *T*-junctions. The red *Y*-junction expresses a convex corner because it is formed from three "+" lines. Varley et al. [21] identified a "cubic corner" based on [15] from a convex *Y*-junction. In their methods, when a *Y*-junction is given in an *x-y* coordinate system and three lines form a cubic corner, their equation can calculate all *z* values of terminals in the lines. Consequently, *Y*-junctions expressing cubic corners in sketches could be converted to 3D cubic corners in 3D models. However, it cannot be applied to ambiguous cuboid sketches such as shown in Fig. 5(a) although people can understand it at a glance. We have searched this human perception for recognizing this figure, and found that people draw sketches as isometric and symmetrical as they can [16]. For example, when a person draw a sketch of a long pole, he/she usually draw it as shown in not Fig. 5(b) but Fig. 5(c) because it is easy to understand the pole exactly for people. Also, people do not usually understand Example 1 as Fig. 2(c). In general, hidden shapes of sketches occur at *T*-junctions. There are several researches for the prediction of the hidden shapes from *T*-junctions. For instance, Cao et al. [2] attempted topological approach although they handled only polyhedrons.
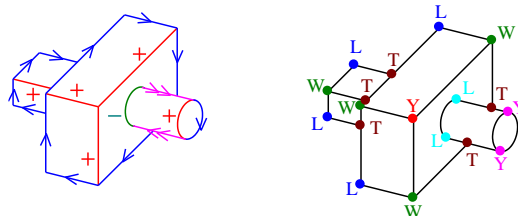


**Figure 4**: Line labeling in Example 1: (a) Line labeling and (b) Junctions.
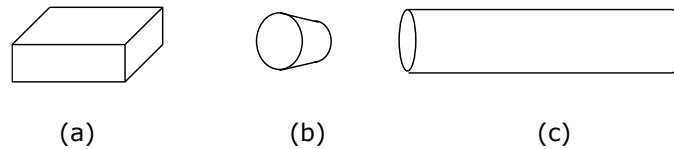
Figure 5: Three types of sketches: (a) Ambiguous but understandable cuboid sketch, (b) A sketch of a long pole, and (c) Another sketch of the pole.

In recent years, Company et al. [7] investigated techniques to detect junctions from sketches using human perception. From this analysis, it can be determined that human perception is important for conversion, which is incorporated in our method. Interactive or semiautomatic systems for conversion were previously proposed, [1],[24]; however, there are no fully automatic systems for conversion. Further, 3D sketching systems were also developed [10-11]. Although these systems might be useful for beginners, they are only a few types of solid modelers, for example, CATIA and SolidWorks. Neural network techniques especially deep learning techniques have also been actively used for conversion [3-4],[9],[13],[20],[22-23]. Although these learning techniques will be effective to find 3D objects from sketches automatically, it will be difficult to convert sketches into 3D models geometrically and precisely. Moreover, the learning will be suitable for known objects such as tables, chairs, cups; however, it is not suitable for different types of mechanical and creative objects because each of them must be learned individually and repeatedly for different cases. The learning of these objects seems to be wasteful. In summary, although all the studies described above are effective for conversion, the types of convertible objects are strictly limited. Our proposed method in this paper aims to extend the limitation of convertible objects significantly more than conventional techniques by predicting hidden shapes of sketches in accordance with human perception.

## 3   ALGORITHM OF THIS METHOD

In this method, all SFs are initially defined. They are quite different from "machining features" in CAD techniques. Firstly, we found that people can recognize and draw simple sketches as shown in Fig. 1, and they can be recognized as 3D models. So, we got an idea that if a complex sketch can be disassembled into these simple sketches, it can be converted to a 3D model. Therefore, we have not referred to machining features and their recognition techniques. This is because finding more effective SFs for the conversion is a more important problem so that the abstraction of SFs is the main theme in this paper. However, abstracted machining features would be meaningless because they cannot be machined. In this method, a sketch is drawn in 2D drawing systems on a PC, tablet, etc. Also, a sketch is an orthogonal and opaque projection of a 3D object placed in a general position. In the present step of this method, main targets of sketches are mechanical parts. In addition, each sketch consists of ellipses, elliptical arcs, and straight lines. Images and freehand sketches are not be handled in this method because this problem can be separated from the conversion. For example, the problem was handled in [1],[8].

The algorithm of this method is shown in Fig. 6. Here, this method is explained using Example 1 shown in Fig. 2(a) in accordance with the algorithm. When Example 1 is input, in Step 1 of the algorithm, straight lines are divided at their intersections. In Step 2, additional lines are drawn as dotted lines. They can be drawn from T-, W-, and L-junctions, such as extending their lines within the input sketch. If a curved line is an element of a T-junction, it is extended in a manner similar to forming an oval. If an additional line cannot become a part of a closed loop of lines, it is cut until the loop is formed. In Example 1, ten additional lines (brown) can be drawn as shown in Fig. 7(a). In Step 3, each region forming a closed loop of line(s) is recognized for detecting an SF. In Step 4, a (red) cylinder sketch can be detected as shown in Fig. 7(b). In Step 6, all useless additional lines are removed, and a hidden (red) elliptical arc can be drawn as an additional line in Step 7 as shown in this figure. Step 8 is omitted at this time. In Step 9, the cylinder sketch can be extracted as a 3D cylinder model ($f_1$) as shown in Fig. 7(c). The dimensions of the $f_1$ are corresponded to the cylinder sketch because of the assumption that sketches are drawn as isometric as possible. In this method,

each extracted SF can be called a 3D feature. After this extraction, the contact face between $f_1$ and the other 3D feature become an (blue) ellipse as shown in this figure. There is an assumption that $f_1$ contacts at its bottom face to the other 3D feature. This assumption can be almost correct in human perception because people usually do not predict that they are separated such as Fig. 2(c). In Step 10, this process goes back to Step 1 because many lines are remained. Continuously, a (red) cuboid sketch can be detected as shown in Fig. 7(d), and a 3D coordinate system can be defined. This definition is explained in the next paragraph. When the cuboid is extracted as a 3D feature ($f_2$), five (green) lines are remained as shown in Fig. 7(e). These lines cannot form any SFs. So, we attempt to abstract SFs. In this method, ASF (Abstract Sketch Feature) is introduced as the first step of this abstraction. Each ASF becomes a cut SF because it is usually occurred at $T$-junction(s). In this figure, five (green) lines can become an ASF of a cuboid sketch in this method. However, the length of the cuboid to $f_2$ cannot be decided at this time. Therefore, we analyze that as follows.
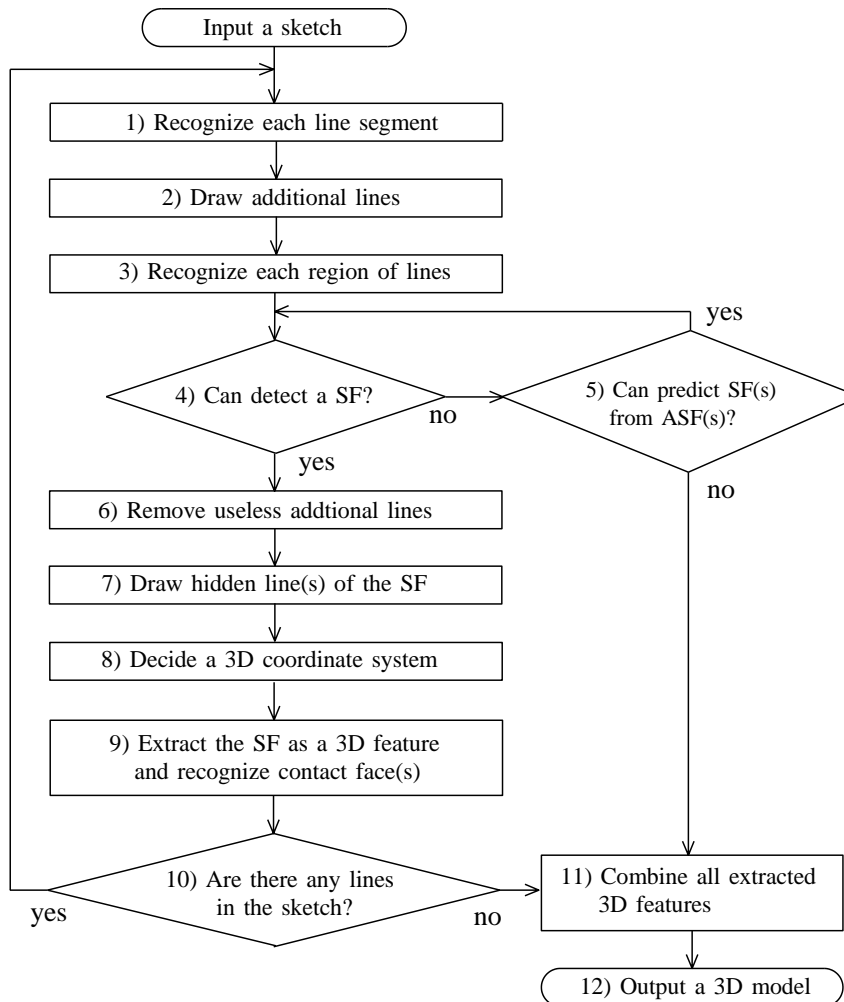


**Figure 6**: The algorithm of this method.

The 3D coordinate system of Example 1 (omitting $f_1$) can be defined from the convex Y-junction of $f_2$ such as shown in Fig. 8(a). In this figure, $P_1P_2$ is one of the lines in the ASF. In Fig. 8(b), $P_1P_2$ is extended as $P_1P_3$. In this figure, the ASF contacts to $f_2$ but their two $T$-junctions are removed.

Therefore, it is found that if $P_1P_3$ is shorter than this figure, they are not contacted. In the same way, if $P_1P_2$ is extended as $P_1P_4$ as shown in Fig. 8(c), the ASF contacts to $f_2$ but if $P_1P_4$ is longer than this figure, they will be overlapped. Therefore, it is found that the length of the line is more than $P_1P_2$ and less than or equal to $P_1P_4$. Here, when a person looks at Example 1, he/she may predict that the ASF contacts to $f_2$ centrally. It is a human perception. In Fig. 8(d), $P_1P_2$ is extended as $P_1P_5$. In this figure, the (brown) contact face of the ASF is placed centrally to $f_2$. This prediction can correspond to that $P_5$ is the middle point between $P_3$ and $P_4$. In general, people prefer to select center/middle points in the range of selective areas because of the human perception. Consequently, an SF of a cuboid as $f_3$ can be defined from the ASF in Step 5. Finally, when three 3D features ($f_1$, $f_2$, $f_3$) can be combined at their contact faces in Step 11, the 3D model of Example 1 can be obtained in Step 12 such as shown in Fig. 2(b). In Fig. 8(e), another SF of a cuboid is drawn to Fig. 8(a). In this case, it is found that the length of $f_3$ is decided as $P_6P_7$ by seeing from y axis. Therefore, it is found that many problems still exist to decide the length of $f_3$.
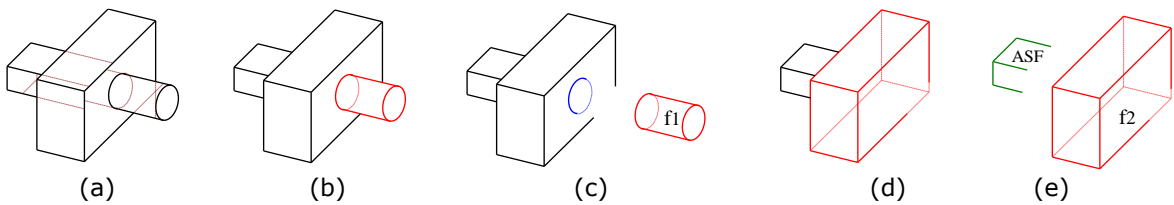


**Figure 7**: The process to convert Example 1 into its 3D model: (a) Drawing of ten additional lines, (b) Detection of an SF of a cylinder, (c) Extraction of the cylinder ($f_1$) and recognition of the contact face of it, (d) Detection of a cuboid, and (e) Extraction of the cuboid ($f_2$) and detection of an ASF of a cuboid.
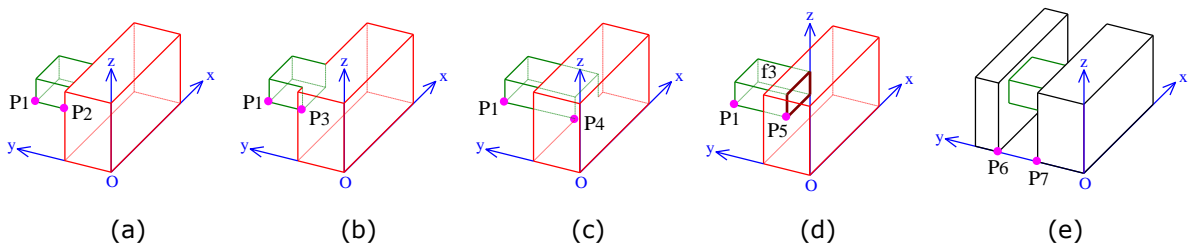


**Figure 8**: The prediction of the length in the ASF: (a) 3D coordinate system, (b) Minimum contact between $f_2$ and ASF, (c) Maximum contact between them, (d) Center contact between them, and (e) A case that ASF contacts to both two cuboids.

Lastly, defined SFs and ASFs in our present step are indicated in Fig. 9 and Fig. 10 respectively. In SFs, three of them are shown in Fig. 1. The other eight SFs are shown in Fig. 9. The detailed explanation of them can be referred in [17-18].
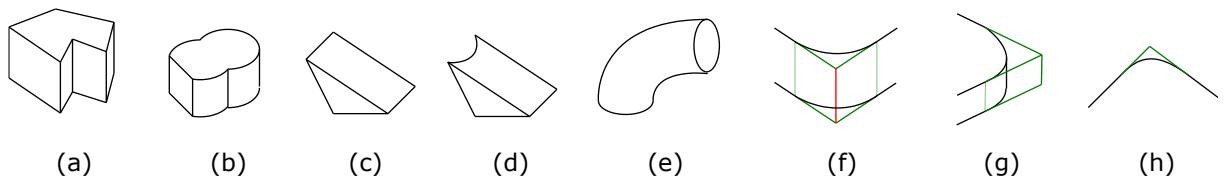


**Figure 9**: Eight SFs: (a) Polygonal extrusion, (b) Multi-extrusion, (c) Rib, (d) Round rib, (e) Pipe, (f) Front fillet, (g) Side fillet, and (h) Hidden fillet.

For example, Fig. 9(a) shows a polygonal extrusion. It consists of a polygon and parallelograms. Fig. 9(b) shows a multi-extrusion. It consists of a multi-region shape, parallelogram(s), and curved parallelogram(s) similar to the polygonal extrusion. Fig. 9(f) shows a front fillet. It consists of four straight lines and two curved lines, and they are contacted tangentially. Also, two green dotted lines can be drawn as additional lines among them. Then four green solid lines can be drawn, and a red line can be drawn as shown in this figure. Consequently, a front fillet sketch can be changed into a polygonal corner sketch.



|       (a)       |       (b)       |       (c)       |       (d)       |       (e)       |       (f)       |       (g)       |
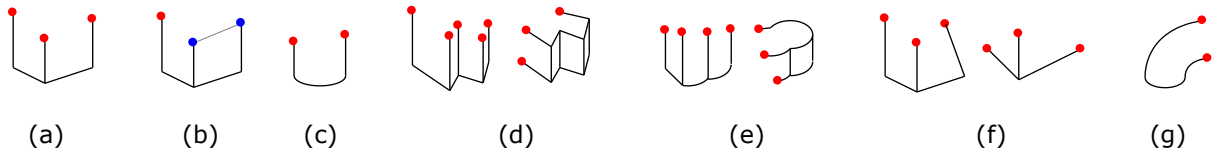
**Figure 10**: Seven types of ASFs: (a) Partial cuboid, (b) Partial cuboid made with an additional line, (c) Partial cylinder, (d) Two types of partial polygonal extrusion, (e) Two types of partial multi-extrusion, (f) Two types of partial rib, and (g) Partial pipe.

Fig. 10(a) shows a partial cuboid. In this figure, each isolated terminal of a line is marked as a red point. Fig. 10(b) shows a partial cuboid with an additional line. In this figure, two terminals of the additional line are blue points because the line becomes an element of a contact face to the other SF. So, these blue points and additional lines can be applied to the other ASFs. Fig. 10(c) shows a partial cylinder. Fig. 10(d) shows two types of partial polygonal extrusion. Fig. 10(e) shows two types of partial multi-extrusion. Fig. 10(f) shows two types of partial rib. Fig. 10(g) shows a partial pipe. These ASFs are representative because obviously there are many more types of ASFs.
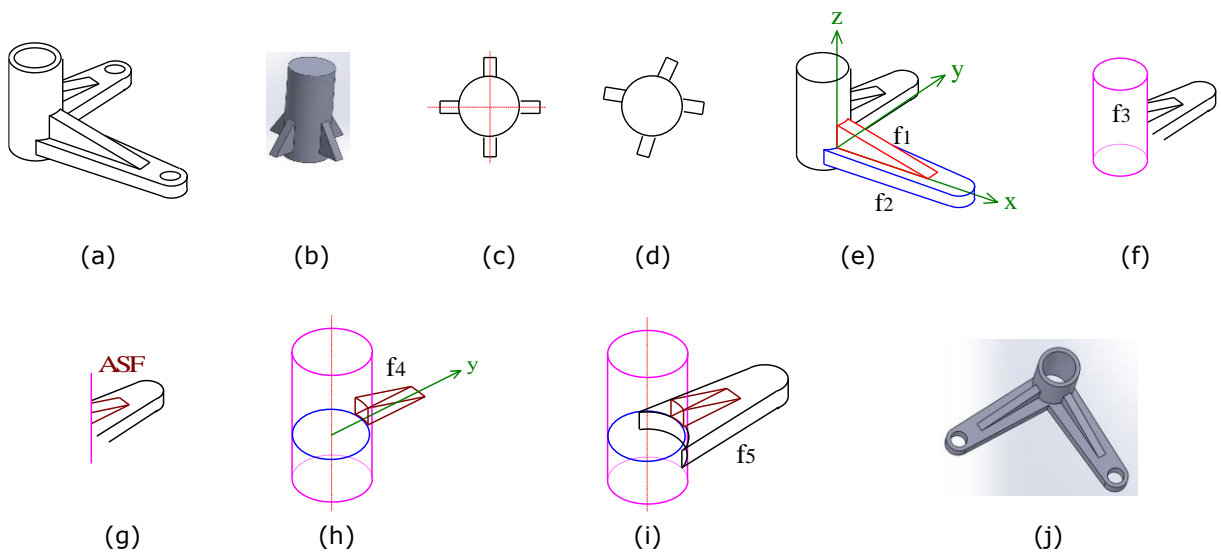
## 4    EXAMPLES

Fig. 11(a) shows Example 2 that is a cylindrical mechanical part. First, an SF of a (red) cylinder can be detected and extracted as $f_1$ as shown in Fig. 11(b). In this case, only $z$ axis can be defined from the axis of $f_1$ as this figure. Second, an SF of a (blue) cylinder can be detected and extracted as $f_2$ as shown in Fig. 11(c). Consequently, a partial (green) cylinder as an ASF can be detected as shown in this figure. When it is assumed that the axis of $f_2$ is the same as the ASF with the human perception, an (green) SF of a cylinder can be predicted as $f_3$ as shown in Fig. 11(d). Consequently, the 3D model of Example 2 can be obtained by combining these three 3D features.



|          (a)          |          (b)          |          (c)          |          (d)          |
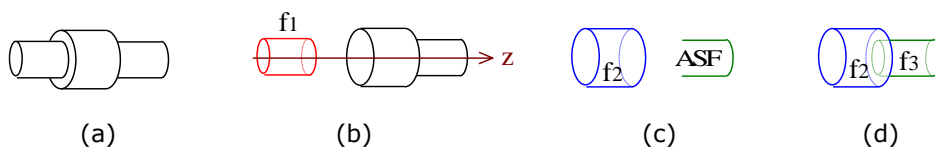
**Figure 11**: Example 2: (a) Example 2, (b) Extraction of $f_1$ and $z$ axis, (c) Extraction of $f_2$ and detection of a partial cylinder as an ASF, and (d) Prediction of $f_3$.

Fig. 12(a) shows Example 3, which is an arm part of a mechanical product. This example was an issue in our last paper [16]. In an overview, this arm seems a cylinder with two ribs. Fig. 12(b) shows a prototype of that. The top view of the prototype can be drawn as shown in Fig. 12(c) in human perception. Therefore, it is found that each rib is placed radially from the axis of the cylinder. In other words, people would not imagine Fig. 12(d) instead of Fig. 12(c). Consequently, people would think that two ribs are placed to the cylinder radially in Example 3. When Example 3 is input to this method, first, three round holes can be detected and extracted as shown in Fig. 12(e).

Second, in this figure, a round (red) rib can be detected and extracted as $f_1$ and then a (blue) multi-extrusion can be detected and extracted as $f_2$ and also a (green) 3D coordinate system can be placed from $f_1$. After $f_1$ and $f_2$ are extracted, a (pink) cylinder can be detected and extracted as $f_3$ as shown in Fig. 12(f). After $f_3$ is extracted, a (brown) partial rib as an ASF can be detected from a (pink) limb line of $f_3$ such as shown in Fig. 12(g). The length of the rib can be predicted by applying the human perception that ribs are placed to a cylinder radially such as Fig. 12(c). The direction of the rib from $f_3$ can be regarded as $y$ axis. So, in Fig. 12(h), the center point of a blue ellipse parallel to two ellipses of $f_3$ is the intersection between the (red) axis of $f_3$ and (green) $y$ axis corresponding to the center line of the bottom face in the rib. Therefore, it is found that the rib can extend until the blue ellipse as this figure so it can become a 3D feature as $f_4$. In the same way, an ASF of a multi-extrusion can be extended in accordance with $f_4$, and it can become $f_5$ as shown in Fig. 12(i). Consequently, the 3D model of Example 3 can be obtained by combining all 3D features as shown in Fig. 12(j).



| (a) | (b) | (c) | (d) | (e) | (f) |



| (g) | (h) | (i) | (j) |

**Figure 12**: Example 3: (a) Example 3, (b) Prototype of a cylinder with ribs, (c) Top view of (b), (d) Unimaginable top view, (e) Detected $f_1$, $f_2$ and placed 3D coordinate system, (f) Extraction of $f_1$, $f_2$ and detected $f_3$, (g) Detection of a partial rib as an ASF, (h) Prediction of $f_4$, (i) Prediction of $f_5$, and (j) Overview of the 3D model of Example 3.

Fig. 13(a) shows Example 4 that is a round table. Obviously, a disk-shaped cylinder can be detected and extracted firstly as shown in Fig. 13(b). However, the lengths of three partial cylinders as ASFs cannot be predicted in the present step of this method. Especially, the prediction of the length in the middle partial cylinder is difficult. In Fig. 13(c), the cylinder is placed at the center of the disk like Example 1, but it is obvious that this placement is a mistake because people know the shapes of tables. It is a normal idea for people that the lengths of the ASFs are the same and they are arranged near the edges of the disk radially in tables. It is difficult to apply this inference to the present step of this method. Although this problem might be solved in pattern recognition techniques of images and/or deep learning techniques, we want to solve that as smarter and more theoretical as possible. One of the measures is a higher abstraction of ASF. If Fig. 13(b) can be defined as a complex ASF, this problem might be solved. So, it would become a next issue for this method.
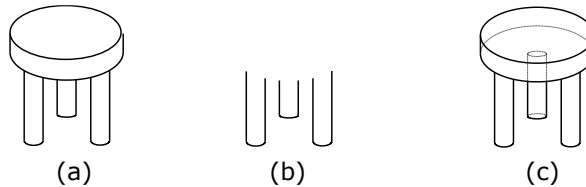
**Figure 13**: Example 4: (a) Example 4, (b) Extracting a disk and appearance of three partial cylinders (ASFs), and (c) Case that middle ASF is contact to the center of the disk.

Fig. 14 shows the algorithm of automatic converting ASFs to SFs in this method. When an ASF in a sketch is input, in Step 1, if there is some contact line, the contact face and the length of the ASF can be confirmed in Step 2, so an SF can be output in Step 7. In Step 3, if some contact face to the ASF can be detected, its length can be decided centrally such as Fig. 8(d) in Step 5 and then Step 7 can be executed. In Step 4, adaptive prototypes such as Fig. 12(b) are searched and applied to find some contact face to the ASF. To find more prototypes and how to apply prototypes to ASFs are the next issues of this method. If this step is failed, "ERROR" is output in Step 6.
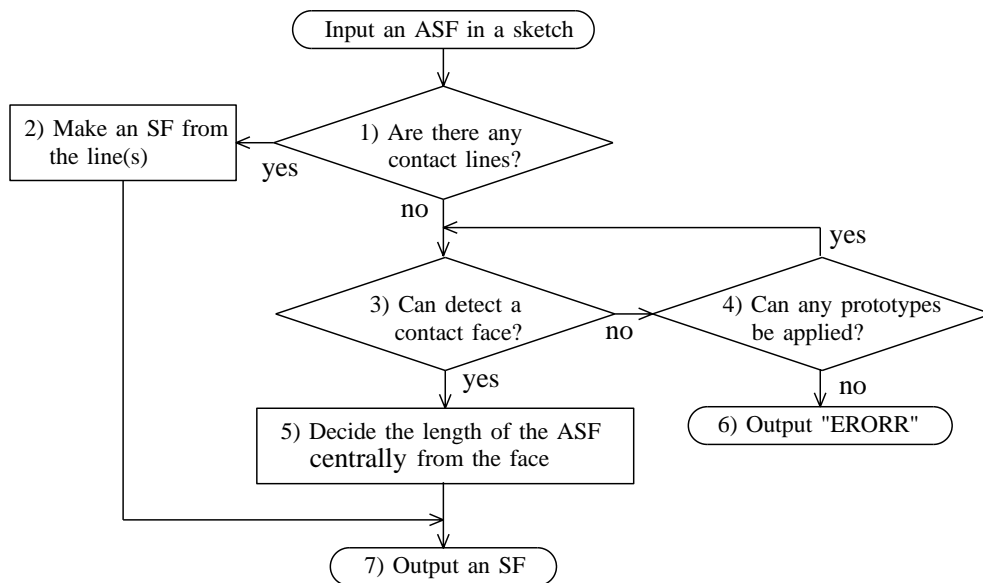


**Figure 14**: The algorithm of automatic converting ASFs to SFs in this method.

## 5   DISCUSSION

Although many issues still exist in the prediction of ASFs, several cases of ASFs can be predicted with human perception in this method in this paper. In Example 1, the length of a partial cuboid as an ASF can be predicted as shown in Fig. 8(d) because of a human perception that people prefer to select center/middle points in the range of selective areas. In Example 3, although the prototype in Fig. 12(b) is introduced, if it is a mistake, it becomes impossible to convert this example into a 3D model such as shown in Fig. 12(j). Therefore, more abstraction (such as Fig. 13(b)) of SFs and clues will be required for this issue in this method. Prototypes such as Fig. 12(b) will become a clue but more adaptive clues would become different views of objects drawn in sketches. The views can be pictures and/or Engineering drawings. In general, the prediction of hidden shapes made from *T*-junctions has been a difficult issue for the researches to automatically convert sketches into 3D models. However, if the issue may be ignored, practical systems for the conversion would never be

developed. Therefore, it is important to research the prediction continuously. On the other hand, it is necessary to make dictionaries of SFs and ASFs. In addition, to handle simplified sketches of mechanical parts will become an issue. For example, Fig. 15 shows sketches of a screw and springs. It is still impossible to handle these sketches in this method despite that there are many mechanical sketches including screws and springs. For the conversion, epochal ASFs would be required.



(a)                    (b)                    (c)
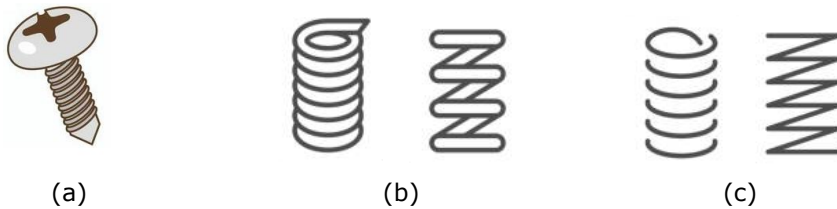
**Figure 15**: Sketches of a screw and springs: (a) Screw, (b) Two types of springs, and (c) Symbolic sketches from (b).

## 6    CONCLUSION

In this paper, a method to predict hidden shapes making from *T*-junctions in sketches by applying human perception is proposed. The results of this method are summarized as follows:

• For this prediction, sketch features (SFs) can be abstracted to ASFs, and seven types of ASFs can be defined, and the algorithm of this method is explained in detail by solving Example 1.

• In Example 1, a partial cuboid as an ASF can be predicted as a SF by human perception that people prefer to select center/middle points in the range of selective areas. Also, a partial cylinder as an ASF can be predicted in Example 2.

• In Example 3, a partial rib and a partial multi-extrusion made from a limb line can be predicted by using a prototype of a cylinder with ribs. Also, it is found that more abstraction of ASF is necessary in Example 4. From these examples, the algorithm of automatic converting ASFs to SFs can be indicated. Consequently, more abstract ASFs, prototypes, and clues such as different views will be required for more exact predictions of hidden shapes in sketches.

• The importance of the prediction is discussed, and to handle simplified sketches such as screws and springs will become an issue.

*Masaji Tanaka*, https://orcid.org/0000-0002-5266-9182
*Tetsuya Asano*, https://orcid.org/0000-0002-4988-6928

## REFERENCES

[1]    Bobenrieth, C.; Cordier, F.; Habibi, A.; Seo, H.: Descriptive: Interactive 3D Shape Modeling from A Single Descriptive Sketch, Computer-Aided Design, 128(102904), 2020, https://doi.org/10.1016/j.cad.2020.102904
[2]    Cao, L.; Liu, J.; Tang, X.: What the back of the object looks like: 3D reconstruction from line drawings without hidden lines, IEEE Transaction on Pattern Analysis and Machine Intelligence, 30(3), 2007, 507–517, https://doi.org/10.1109/TPAMI.2007.1185
[3]    Chen, Q.; Nguyen, V.; Han, F.; Kiveris, R.; Tu, Z.: Topology-Aware Single-Image 3D Shape Reconstruction, Proceedings of the IEEE/CVF Conference on Computer Vision and Pattern Recognition (CVPR) Workshops, 2020, 270-271, https://doi.org/10.1109/CVPRW50498.2020.00143
[4]    Choy, C; Xu, D.; Gwak, J.; Chen, K.; Savarese, S.: 3D-R2N2: A Unified Approach for Single and Multi-view 3D Object Reconstruction, Computer Vision – ECCV, 2016, 628-644, https://doi.org/10.1007/978-3-319-46484-8_38

[5]    Clowes, M.B.: On seeing things, Artificial Intelligence, 2(1), 1971, 79–116. https://doi.org/10.1016/0004-3702(71)90005-1

[6]    Company, P.; Piquer, A.; Contero, M.; Naya, F.: A survey on geometrical reconstruction as a core technology to sketch-based modeling, Computers & Graphics, 29(6), 2005, 892–904, https://dx.doi.org/10.1016/j.cag.2005.09.007

[7]    Company, P.; Plumed, R.; Varley, P. A. C.; Camba, J. D.: Algorithmic Perception of Vertices in Sketched Drawings of Polyhedral Shapes, ACM Transactions on Applied Perception, 16(3), 2019, Article 18, https://doi.org/10.1145/3345507

[8]    Dematapitiya, S.; Kawazoe, M.; Nishikawa, A; Sakurai, M.; Saga, S.: Snapping of fuzzy objects using the multi-resolution fuzzy grid snapping technique, Information and Media Technologies, 4(2), 2009, 463-474. https://doi.org/10.2197/ipsjjip.17.47

[9]    Guo, T.; Cui, R.; Qin, X.; Wang, Y.; Tang, Z.: Bottom-up/top-down geometric object reconstruction with CNN classification for mobile education, PG '18: Proceedings of the 26th Pacific Conference on Computer Graphics and Applications, 2018, 13-16,

[10]   http://help.solidworks.com/2021/English/SolidWorks/sldworks/c_3d_sketching_top.htm

[11]   https://www.sketchup.com/

[12]   Huffman, D. A.: Impossible objects as nonsense sentences, Machine Intelligence 6, 1971, 295–323.

[13]   Jiang, L.; Shi, S.; Qi, X.; Jia, J.: GAL: Geometric Adversarial Loss for Single-View 3D-Object Reconstruction, Proceedings of the European Conference on Computer Vision (ECCV), 2018, 802-816, https://doi.org/10.1007/978-3-030-01237-3_49

[14]   Malik, J.: Interpreting line drawings of curved objects, International Journal of Computer Vision, 1, 1987, 73–103. https://dx.doi.org/10.1007/BF00128527

[15]   Perkins, D. N.: Cubic Corners, Quarterly Progress Report 89, MIT Research Laboratory of Electronics, 1968, 207–214.

[16]   Tanaka, M.; Asano, T.; Higashino, C.: Isometric Conversion of Mechanical Sketches into 3D Models, 18(4), 2021, 772-785, https://doi.org/10.14733/cadaps.2021.772-785

[17]   Tanaka, M.; Kaneeda, T.: Feature extraction from sketches of objects, Computer-Aided Design & Applications, 12(3), 2014, 300-309. https://dx.doi.org/10.1080/16864360.2014.981459

[18]   Tanaka, M.; Terano, M.; Asano, T.; Higashino, C.: Method to Automatically Convert Sketches of Mechanical Objects into 3D Models, Computer-Aided Design & Applications, 17(6), 2020, 1168-1176, https://doi.org/10.14733/cadaps.2020.1168-1176

[19]   Tanaka, M.; Terano, M.; Higashino, C.; Asano, T.; Takasugi, K.: A Learning Method for Reconstructing 3D Models from Sketches, Computer-Aided Design & Applications, 16(6), 2019, 1158-1170, https://doi.org/10.14733/cadaps.2019.1158-1170

[20]   Tatarchenko, M.; Richter, S.; Ranftl, R.; Li, Z.; Koltun, V.; Brox, T: What Do Single-View 3D Reconstruction Networks Learn?, Proceedings of the IEEE/CVF Conference on Computer Vision and Pattern Recognition (CVPR), 2019, 3405-3414, https://doi.org/10.1109/CVPR.2019.00352

[21]   Varley, P. A. C.; Martin, R. R.; Suzuki, H.: Frontal geometry from sketches of engineering objects: is line labelling necessary?, Computer-Aided Design, 37(12), 2005, 1285–1307, https://doi.org/10.1016/j.cad.2005.01.002

[22]   Yang, B.; Wen, H.; Wang, S.; Clark, R.; Markham, A.; Trigoni, N.: 3D Object Reconstruction from a Single Depth View with Adversarial Learning, Proceedings of the IEEE International Conference on Computer Vision (ICCV), 2017, 679-688, https://doi.org/10.1109/ICCVW.2017.86

[23]   Yang, B.; Rosa, S.; Markham, A.; Trigoni, N.; Wen, H.: Dense 3D Object Reconstruction from a Single Depth View, IEEE Transactions on Pattern Analysis and Machine Intelligence, 41(12), 2019, https://doi.org/10.1109/TPAMI.2018.2868195

[24]   Zou, C.; Peng, X.; Lv, H.; Chen, S.; Fu, H.; Liu, J.: Sketch-based 3-D modeling for piecewise planar objects in single images, Computers & Graphics, 46, 2015, 130-137, https://doi.org/10.1016/j.cag.2014.09.031